

SEARCH FOR STABLE ORBITS AROUND 1999 KW4

Thais C. Oliveira* and Antonio F. B. A. Prado†

This paper is a study of the orbital motion of a space vehicle around the binary system 1999 KW4. The model used is the restricted full body problem, in which it is assumed that the mass of the spacecraft is negligible and that the binary system is composed of two-ellipsoid bodies. The equations of motion of the binary system are found using Lagrange's method. The solar radiation pressure perturbation is assumed to act on the spacecraft's dynamics along with the gravitational influence of the non-spherical asteroid bodies. The results are based on a grid search method to find stable orbits for a spacecraft to visit the 1999 KW4 system. Several types of families of orbits are found, such as orbits around one or both asteroid bodies. Trajectories ending in escapes from the double system or collisions with one of the asteroid bodies are also mapped because they need to be avoided. The eccentricity of the orbit of the binary system around the Sun is approximately 0.69, a large value, therefore the effect of the solar radiation pressure on the orbit of the spacecraft for short and long periods is investigated.

INTRODUCTION

Asteroids are fascinating objects in the solar system. They are an important key to understanding the formation of the solar system because they are nearly unaltered remains of the solar nebula from approximately 4.6 billion years ago.¹

Asteroids are rocky or metallic airless objects from the Solar system that are too small to be called planets. They come in different shapes and sizes, e.g., Vesta is the largest known asteroid at approximately 530 kilometers in diameter (see Reference 2) and 2015 TC25 is the smallest known asteroid at approximately 2 meters in diameter.^{3,4} A few massive asteroids are nearly spherical, while most asteroids do not have enough mass become a nearly spherical and thus have irregular shapes. Because asteroids do not have enough mass and magnetic field to contain an atmosphere, the airless bodies are covered in craters.

NEAs (Near-Earth Asteroids) are a group of asteroids that approach the Earth's orbital distance to within 45 million km and they can pose an impact danger to Earth. The probability of an impact is low, but the consequences could be catastrophic depending on the size and velocity of the object. Such hazard events have occurred before on Earth, e.g., the mass extinction 65 million years ago caused by a massive asteroid impact.⁵ Thus, it is not surprising that asteroids can be an alarming potential threat that should be studied in advance in order to mitigate a potential impact. Several spacecraft missions have been envisaged to explore asteroids, binary asteroid systems, triple asteroid systems. Some missions to explore these bodies have already occurred and been successful in gathering real data.^{6,7,8,9}

Since the discovery of the first known binary system, 243 Ida [see Reference 10], numerous binary systems, including Near-Earth Asteroids (NEAs), have been observed in the Solar System. 309 binary asteroids

* Space Mechanic and Tecnology, INPE/National Institute for Space Research, Av. dos Astronautas 1.758, SJC-SP, 12227-010, Brazil. E-mail: thais.oliveira@inpe.br

† Space Mechanic and Tecnology, INPE/National Institute for Space Research, Av. dos Astronautas 1.758, SJC-SP, 12227-010, Brazil. E-mail: antonio.prado@inpe.br

systems have been discovered thus far: 63 NEAs, 24 Mars crossing asteroids, 140 main-belt asteroids, 4 Jupiter Trojans and 78 trans-Neptunian objects.¹¹

Binary and multiple systems are frequent among asteroids smaller than 15 km in diameter of the primary body.¹² According to photometrically detected binaries systems, an estimate suggests the upper limit of the primary body diameter to be approximately 13 km.¹³

Current estimates indicate that the fraction of binaries in the population of NEAs that are larger than 300 m in diameter is $15 \pm 4\%$.¹⁴

The binary asteroid system studied in this paper is the (66391) 1999 KW4. It is classified as a Near-Earth object and potentially hazardous asteroid. It is a Mercury-crosser and the closest known binary system to the Sun with a perihelion of just 0.2 AU. It was discovered on 20th May 1999, by Lincoln Near-Earth Asteroid Research at the Lincoln Laboratory's Experimental Test Site in Socorro, New Mexico, United States.¹⁵ In 2006 it was revealed to be a binary system.¹⁶

This binary asteroid system was selected for study because of its proximity to the Sun. The spacecraft's orbit is highly perturbed by the solar radiation pressure at the perihelion of the orbit and that is why this binary system is a potential hazardous NEA. Furthermore, this binary system's physical properties and dynamics have been well studied in the literature review, thus, there is a lot data and analysis on this binary system's dynamics.^{17,18,19}

The focus of this paper is to find stable spacecraft orbits around the binary asteroid system KW4. The solar radiation pressure is considered as an external perturbation force of the spacecraft's dynamics. The non-spherical nature of the binary system is also considered in the orbital dynamics of the spacecraft and the binary system itself.

In the following section - Mathematical Formulation - the dynamics of the binary system based on the two-ellipsoid model and the motion of spacecraft in the gravitational field is analytically described in more detail. In the results section, the search for stable orbits is performed using two techniques: a grid search that assumes different initial Keplerian Orbital elements around the primary body; and utilization of the Jacobi constant and orbits near equilibrium points to find an initial state before performing a grid search discover to find which orbits do not collide or escape the system for different Jacobi constants.

MATHEMATICAL FORMULATION

This section provides the mathematical formulation of the solar radiation pressure force model of the spacecraft, the dynamics of the binary asteroid system and the spacecraft's orbital motion around the binary system. Additionally, the mathematical formulation of zero velocity curves based on the Jacobi constant of a circular mutual orbit of binary asteroid bodies.

Solar Radiation Pressure Force Modelling

The influence of the solar radiation pressure is more pronounced in interplanetary missions where the spacecraft is under the sphere of influence of a weak gravitational field and negligible atmospheric drag, e.g., spacecraft orbiting around the Sun, asteroids or small natural satellites is given.

The solar radiation pressure comes from the momentum exchange upon the interaction of a flux of photon-particles with the spacecraft's surface.

In this work, the absorptivity, the specular reflectivity and the diffuse reflectivity of the spacecraft's surface are considered. Their respective coefficients are given by: β , ρ , δ . The sum of these coefficients is equal to one, i.e., $\beta + \rho + \delta = 1$. The model assumes Lambertian reflection, which means that the reflection can be described in terms of specular and diffuse reflectivities.²⁰ The absorbed energy is assumed to not be reemitted. The specular reflection is perfectly specular. In other words, the spacecraft's surface behaves like a linear combination of a black body, a perfect mirror, and a Lambertian diffuser.²¹

The spacecraft's surface is modeled as a rectangular prism with flat plates. The assumed orientation of the spacecraft is that one of its faces is always turned toward the primary asteroid body. The area of the spacecraft is considered to be 25 m² with a mass of 500 kg.

The mathematical formulation for the force due to solar radiation pressure acting on each of the spacecraft's flat surfaces is given by: ^{20, 21, 22, 23}

$$\mathbf{F} = \frac{\phi A \cos \theta}{c} \left[(1 + \rho) \hat{\mathbf{s}} + 2 \left(\frac{\delta}{3} + \rho \cos \theta \right) \hat{\mathbf{n}} \right] \quad (1)$$

where \mathbf{F} is the force due to solar radiation pressure on a flat plate [N]; A is the surface area of the flat surface [m^2], θ is the angle between the surface normal and spacecraft to Sun vectors; $\hat{\mathbf{s}}$ is the spacecraft to Sun unit vector and $\hat{\mathbf{n}}$ is the surface normal vector.

Physical and Orbital Parameters of 1999 KW4

Table 1 and Table 2 present some physical and orbital parameters of the 1999 KW4 system. It is assumed that the inclination, ascending node and argument of perigee are zeroed for the secondary asteroid body around the primary in Table 2.

Table 1. Physical Parameters of the 1999 KW4 Asteroid Bodies.

	Asteroid 1	Asteroid 2
Dimensions	1.532 x 1.495 x 1.347 km	0.571 x 0.463 x 0.349 km
Mass	2.353 10^{12} kg	0.135 10^{12} kg
Spin Rate	2.7645 hr	17.4 hr

Table 2. Orbital Data for the 1999 KW4 Asteroid Bodies.

	Primary	Secondary
Semi-major axis	0.642291859 au	2.548 km
Eccentricity	0.688460238	0.0004
Inclination	105.4°	0°
Ascending Node	244.9231238°	0°
Argument of Peri- gee	192.6154467°	0°

The Binary Asteroid System Dynamics

This paper considers a two-ellipsoid binary system for the 1999 KW4. The mass of the primary body is m_1 and the mass of the secondary body is m_2 . The mass of the Sun is m_{Sun} and treated as a point mass. The inertial reference frame $O_{Sun}XYZ$ is located at m_{Sun} (O_{Sun}) along with the unit vectors \hat{X} , \hat{Y} and \hat{Z} .

The center of mass of the binary asteroid body is located at O and its position vector, with respect to the inertial reference frame, is \mathbf{R}_0 . The axes xyz form the local reference frame, with its origin attached to O . The x axis is oriented along the line that connects the binary asteroid system. The unit vectors of the $Oxyz$ local reference frame are given by \hat{x} , \hat{y} and \hat{z} . The orientation of the local reference frame relative to the inertial frame is given by the angle θ .

The center of mass of each ellipsoid body is given by O_1 and O_2 . The position vectors of each center of mass with respect to the inertial reference frame are \mathbf{R}_1 and \mathbf{R}_2 . A body fixed frame is defined for each body given by $O_1x_1y_1z_1$ for the primary body and $O_2x_2y_2z_2$ for the secondary body. The unit vectors of the body fixed frame are $\hat{x}_i, \hat{y}_i, \hat{z}_i$, for $i = 1, 2$. The orientation of the asteroid body i with respect to its body fixed

frame is given by the angle α_i , i.e., the asteroid bodies rotate in the same direction as the orbital plane's rotation.

Figure 1 illustrates the binary asteroid system geometry with the angles α_1 , α_2 and θ , the position vectors \mathbf{R}_0 , \mathbf{R}_1 , \mathbf{R}_2 and \mathbf{R}_{12} and the reference frames $O_{Sun}XYZ$, $Oxyz$, $O_1x_1y_1z_1$ and $O_2x_2y_2z_2$.²⁴

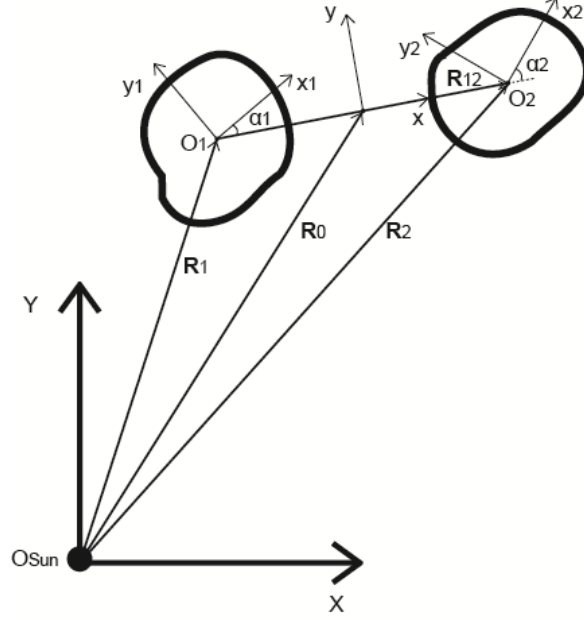


Figure 1. Two-ellipsoid asteroid bodies geometry.

It is assumed that the body-fixed frame $O_i x_i y_i z_i$ is aligned with the principal axes, i.e., the inertia matrix is diagonal and expressed as:

$$\mathbf{I}_i = \begin{bmatrix} I_{xxi} & 0 & 0 \\ 0 & I_{yyi} & 0 \\ 0 & 0 & I_{zz i} \end{bmatrix} \quad (2)$$

where I_{xxi} , I_{yyi} and $I_{zz i}$ are the moments of inertia with respect to the $x_i y_i z_i$ axes, for $i = 1, 2$.

The binary system can be described by four generalized coordinates: the distance R_{12} between O_1 and O_2 ; the local reference frame angle orientation θ with respect to the inertial frame, and the local orientation angles α_1 and α_2 of the asteroid bodies.

The Lagrange's equation is given by:

$$\frac{d}{dt} \frac{\partial T}{\partial \dot{q}_j} - \frac{\partial T}{\partial q_j} + \frac{\partial U}{\partial q_j} = 0 \quad (3)$$

where q_j is the generalized coordinates R_{12} , θ , α_1 and α_2 .

The equations of motion are given by:²⁴

$$\begin{aligned} \ddot{R}_C - R_C \dot{\theta}^2 + \frac{G(m_1 + m_2)}{R_C^2} \\ + \frac{3G(m_1 + m_2)}{4R_C^2} \left\{ \frac{1}{m_1} [2I_{zz1} - I_{xx1} - I_{yy1} + 3(2I_{yy1} - 2I_{xx1}) \cos 2\alpha_1] \right. \\ \left. + \frac{1}{m_2} [2I_{zz2} - I_{xx2} - I_{yy2} + 3(2I_{yy2} - 2I_{xx2}) \cos 2\alpha_2] \right\} = 0 \end{aligned} \quad (4)$$

$$\frac{d}{dt} \left\{ R_{12}^2 \dot{\theta} \frac{m_1 + m_2}{m_1 m_2} [I_{zz1}(\dot{\theta} + \dot{\alpha}_1) + I_{zz2}(\dot{\theta} + \dot{\alpha}_2)] \right\} = 0 \quad (5)$$

$$I_{zz1}(\ddot{\theta} + \ddot{\alpha}_1) + \frac{3Gm_2}{2R_{12}^3} (I_{yy1} - I_{xx1}) \sin 2\alpha_1 = 0 \quad (6)$$

$$I_{zz2}(\ddot{\theta} + \ddot{\alpha}_2) + \frac{3Gm_1}{2R_{12}^3} (I_{yy2} - I_{xx2}) \sin 2\alpha_2 = 0 \quad (7)$$

Radii of Gyration of an Ellipsoid

The radii of gyration of any body shape can be obtained with its mass and its integral moments of inertia.

The mass of an ellipsoid with dimensions ar_0, br_0, cr_0 in the x, y, z directions is:

$$m = \frac{4}{3} \rho \pi abc r_0^3 \quad (8)$$

The moments of inertia are:

$$I_{xx} = \frac{1}{5} m (b^2 r_0^2 + c^2 r_0^2) \equiv m r_{xx}^2 \quad (9)$$

$$I_{yy} = \frac{1}{5} m (a^2 r_0^2 + c^2 r_0^2) \equiv m r_{yy}^2 \quad (10)$$

$$I_{zz} = \frac{1}{5} m (a^2 r_0^2 + b^2 r_0^2) \equiv m r_{zz}^2 \quad (11)$$

where r_{xx}, r_{yy}, r_{zz} are the radii of gyration.

Nondimensional Variables

The distance, mass and time variables are nondimensionalized. The distance variable is nondimensionalized by the characteristic length of the mutual orbits given by l . The characteristic length of the bodies is r_0 .

Let $\epsilon = \left(\frac{r_0}{l}\right)^2$.²⁴

The moments of inertia are re-written in terms of the nondimensionalized radii of gyration by:

$$p_{xxi}^2 = \frac{I_{xxi}}{\epsilon m_i l^2}; p_{yyi}^2 = \frac{I_{yyi}}{\epsilon m_i l^2}; p_{zz_i}^2 = \frac{I_{zz_i}}{\epsilon m_i l^2} \quad (12)$$

where $p_{xxi}, p_{yyi}, p_{zz_i}$ for $i = 1, 2$.

Let the time t be nondimensionalized by $\tau = nt$, where $n \equiv \left(\frac{G(m_1+m_2)}{l^3}\right)^{\frac{1}{2}}$ and G be the gravitational constant. In fact, n is the angular velocity of a body moving in a circular orbit with radius l .

The time derivatives of t and the nondimensional time τ are given as follows:

$$(\dot{\cdot}) \equiv \frac{d(\cdot)}{dt} = n \frac{d(\cdot)}{d\tau} \quad (13)$$

The generalized variable R_{12} is also changed to the nondimensional variable u as follows:

$$u \equiv \frac{l}{R_{12}} \quad (14)$$

The equations of motion after the nondimensionalization are given as follows:²⁴

$$\frac{d^2 u}{d\tau^2} - u \frac{d\theta}{d\tau} - u^4 - \epsilon \frac{3}{4} u^6 (k_{12}^2 + 3k_1^2 \cos 2\alpha_1 + 3k_2^2 \cos 2\alpha_2) = 0 \quad (15)$$

$$\frac{d\theta}{d\tau} - \frac{h}{nl^2} + \epsilon u^2 \left[\frac{p_{zz1}}{1-v} \left(\frac{d\theta}{d\tau} - \frac{d\alpha_1}{d\tau} \right) + \frac{p_{zz2}}{v} \left(\frac{d\theta}{d\tau} - \frac{d\alpha_2}{d\tau} \right) \right] = 0 \quad (16)$$

$$\frac{d^2\theta}{d\tau^2} + \frac{d^2\alpha_1}{d\tau^2} + \frac{3}{2}(1-v) \frac{k_1^2}{p_{zz1}^2} u^4 \sin 2\alpha_1 = 0 \quad (17)$$

$$\frac{d^2\theta}{d\tau^2} + \frac{d^2\alpha_2}{d\tau^2} + \frac{3}{2}v \frac{k_2^2}{p_{zz2}^2} u^3 \sin 2\alpha_3 = 0 \quad (18)$$

where h is the constant of integration of Eq. (16). The constant h can be understood as the angular momentum of the mutual orbits.

Energetic and Hill Stability

The energetically stable relative equilibria and conditions for Hill stability are determined for the two-ellipsoid binary asteroid system.²⁵

The energetic stability determines whether the system can seek out a lower energy state by dissipation of energy. An energetically stable system is a system that has reached its lowest energy state for a given angular momentum.

The Hill stability determines whether the system can undergo a mutual escape. A Hill stable system means the asteroid bodies will not escape the mutual orbit as it evolves dynamically.

The condition for the energetic stability is:²⁵

$$u_{max}^2 < \frac{1}{\epsilon} \left[\frac{3}{2} \left\{ \frac{p_{zz1}^2}{1-v} + \frac{p_{zz2}^2}{v} + \frac{\gamma}{2} \right\} + \frac{1}{2} \left(9 \left\{ \frac{p_{zz1}^2}{1-v} + \frac{p_{zz2}^2}{v} + \frac{\gamma}{2} \right\}^2 + 30\gamma \left(\frac{p_{zz1}^2}{1-v} + \frac{p_{zz2}^2}{v} \right) \right)^{1/2} \right]^{-1} \quad (19)$$

where u_{max} is the maximum u value or the minimum R_{12} distance between the asteroid bodies and $\gamma = p_{zz1}^2 - 2p_{xx1}^2 + p_{yy1}^2 + p_{zz2}^2 - 2p_{xx2}^2 + p_{yy2}^2$.

The condition for the Hill stability is given [Reference 25]:

$$u_{min}^2 < \frac{2}{\epsilon} \left[\frac{p_{zz1}^2}{1-v} + \frac{p_{zz2}^2}{v} + \frac{\gamma}{2} \right]^{-1} \left[1 + \left(1 + \left\{ 6\gamma \left(\frac{p_{zz1}^2}{1-v} + \frac{p_{zz2}^2}{v} \right) \right\} \left[\frac{p_{zz1}^2}{1-v} + \frac{p_{zz2}^2}{v} + \gamma \right]^{-2} \right)^{1/2} \right]^{-1} \quad (20)$$

Spacecraft's Equations of Motion

Let \mathbf{R} be the spacecraft's position vector with respect to the local reference frame Oxyz. Let the spacecraft's position vector \mathbf{R}_{13} and \mathbf{R}_{23} be from the asteroid bodies center of mass m_1 and m_2 , respectively. The nondimensionalization of the position vectors \mathbf{R} , \mathbf{R}_{13} and \mathbf{R}_{23} is given by:

$$\mathbf{r} = \frac{\mathbf{R}}{l} = x\hat{\mathbf{x}} + y\hat{\mathbf{y}} + z\hat{\mathbf{z}} \quad (21)$$

$$\mathbf{r}_{13} = \frac{\mathbf{R}_{13}}{l} = \left(\frac{1-v}{u} + x \right) \hat{\mathbf{x}} + y\hat{\mathbf{y}} + z\hat{\mathbf{z}} \quad (22)$$

$$\mathbf{r}_{23} = \frac{\mathbf{R}_{23}}{l} = x \left(\frac{-v}{u} + x \right) + y\hat{\mathbf{y}} + z\hat{\mathbf{z}} \quad (23)$$

The nondimensional equations of motion of the spacecraft around the binary system are given by:

$$\frac{d^2x}{d\tau^2} - y \frac{d^2\theta}{d\tau^2} - 2 \frac{d\theta}{d\tau} \frac{dy}{d\tau} - x \left(\frac{d\theta}{d\tau} \right)^2 = f_1(x, y, z, u, \alpha_1, \alpha_2) \quad (24)$$

$$\frac{d^2y}{d\tau^2} + x \frac{d^2\theta}{d\tau^2} + 2 \frac{d\theta}{d\tau} \frac{dx}{d\tau} - y \left(\frac{d\theta}{d\tau} \right)^2 = f_2(x, y, z, u, \alpha_1, \alpha_2) \quad (25)$$

$$\frac{d^2z}{d\tau^2} = f_3(x, y, z, u, \alpha_1, \alpha_2) \quad (26)$$

where

$$\begin{aligned} f_1(x, y, z, u, \alpha_1, \alpha_2) = & -v \left(\left\{ \frac{1}{r_{13}^2} \right. \right. \\ & + \frac{3}{2r_{13}^2} \epsilon \left[2(p_{xx1}^2 + p_{yy1}^2 + p_{zz1}^2) - \frac{5}{r_{13}^2} (a_1^2 p_{xx1}^2 + b_1^2 p_{yy1}^2 + c_1^2 p_{zz1}^2) \right] \left. \right\} \left(\frac{1-v}{u} + x \right) \\ & + \frac{3}{2r_{13}^2} \epsilon [a_1(-p_{xx1}^2 + p_{yy1}^2 + p_{zz1}^2) \cos \alpha_1 - b_1(p_{xx1}^2 - p_{yy1}^2 + p_{zz1}^2) \sin \alpha_1] \end{aligned} \quad (27)$$

$$\begin{aligned} (1-v) \left(\left\{ \frac{1}{r_{23}^2} + \frac{3}{2r_{23}^2} \epsilon \left[2(p_{xx2}^2 + p_{yy2}^2 + p_{zz2}^2) - \frac{5}{r_{23}^2} (a_2^2 p_{xx2}^2 + b_2^2 p_{yy2}^2 + c_2^2 p_{zz2}^2) \right] \right\} \left(\frac{-v}{u} + x \right) \right. \\ \left. + \frac{3}{2r_{23}^2} \epsilon [a_2(-p_{xx2}^2 + p_{yy2}^2 + p_{zz2}^2) \cos \alpha_2 - b_2(p_{xx2}^2 - p_{yy2}^2 + p_{zz2}^2) \sin \alpha_2] \right) \end{aligned}$$

$$\begin{aligned} f_2(x, y, z, u, \alpha_1, \alpha_2) = & -v \left(\left\{ \frac{1}{r_{13}^2} + \frac{3}{2r_{13}^2} \epsilon \left[2(p_{xx1}^2 + p_{yy1}^2 + p_{zz1}^2) - \frac{5}{r_{13}^2} (a_1^2 p_{xx1}^2 + b_1^2 p_{yy1}^2 + c_1^2 p_{zz1}^2) \right] \right\} y \right. \\ & \left. + \frac{3}{2r_{13}^2} \epsilon [a_1(-p_{xx1}^2 + p_{yy1}^2 + p_{zz1}^2) \sin \alpha_1 + b_1(p_{xx1}^2 - p_{yy1}^2 + p_{zz1}^2) \cos \alpha_1] \right) \end{aligned} \quad (28)$$

$$\begin{aligned} -(1-v) \left(\left\{ \frac{1}{r_{23}^2} + \frac{3}{2r_{23}^2} \epsilon \left[2(p_{xx2}^2 + p_{yy2}^2 + p_{zz2}^2) - \frac{5}{r_{23}^2} (a_2^2 p_{xx2}^2 + b_2^2 p_{yy2}^2 + c_2^2 p_{zz2}^2) \right] \right\} y \right. \\ \left. + \frac{3}{2r_{23}^2} \epsilon [a_2(-p_{xx2}^2 + p_{yy2}^2 + p_{zz2}^2) \sin \alpha_2 + b_2(p_{xx2}^2 - p_{yy2}^2 + p_{zz2}^2) \cos \alpha_2] \right) \end{aligned}$$

$$\begin{aligned} f_3(x, y, z, u, \alpha_1, \alpha_2) = & -v \left(\left\{ \frac{1}{r_{13}^2} + \frac{3}{2r_{13}^2} \epsilon \left[2(p_{xx1}^2 + p_{yy1}^2 + p_{zz1}^2) - \frac{5}{r_{13}^2} (a_1^2 p_{xx1}^2 + b_1^2 p_{yy1}^2 + c_1^2 p_{zz1}^2) \right] \right\} z \right. \\ & \left. + \frac{3}{2r_{13}^2} \epsilon c_1 (p_{xx1}^2 + p_{yy1}^2 - p_{zz1}^2) \right) \end{aligned} \quad (29)$$

where

$$a_1 = -\left(\frac{1-v}{u} + x \right) \cos \alpha_1 - y \sin \alpha_1; \quad a_2 = -\left(\frac{-v}{u} + x \right) \cos \alpha_2 - y \sin \alpha_2;$$

$$b_1 = \left(\frac{1-v}{u} + x \right) \sin \alpha_1 - y \cos \alpha_1; \quad b_2 = \left(\frac{-v}{u} + x \right) \sin \alpha_2 - y \cos \alpha_2;$$

$$c_1 = c_2 = -z.$$

Jacobi Constant and Mutual Circular Orbit

The Jacobi constant and zero velocity curves can be useful for finding large periodic orbits of a spacecraft that is orbiting around a binary system with a circular mutual orbit.

If the orbit of the binary asteroid system can be approximated to a circular mutual orbit, then $u(\tau) = u_c$ and $\frac{d\theta}{d\tau} = \frac{d\theta}{d\tau} \Big|_c$, where the sub-index c means that the variable is a constant. The equations of motion given by Eqs. (24),(25) and (26) can be re-written as:

$$\frac{d^2x}{d\tau^2} - 2 \frac{d\theta}{d\tau} \Big|_c \frac{dy}{d\tau} = \frac{\partial \tilde{U}}{\partial x} \quad (30)$$

$$\frac{d^2y}{d\tau^2} + 2 \frac{d\theta}{d\tau} \Big|_c \frac{dx}{d\tau} = \frac{\partial \check{U}}{\partial y} \quad (31)$$

$$\frac{d^2z}{d\tau^2} = \frac{\partial \check{U}}{\partial z} \quad (32)$$

where $\check{U} = \frac{1}{2} \frac{d\theta}{d\tau} \Big|_c (x^2 + y^2) + v \left\{ \frac{1}{r_{13c}} + \epsilon \frac{3}{2r_{13c}^3} \left[\frac{p_{xx1}^2 + p_{yy1}^2 + p_{zz1}^2}{3} - \left(\frac{1-v}{u_c} + x \right)^2 \frac{p_{xx1}^2 + p_{yy1}^2 + p_{zz1}^2}{r_{13c}^2} \right] \right\}$

The Jacobi integral can be expressed as:

$$C \left(x, y, z, \frac{dx}{d\tau}, \frac{dy}{d\tau}, \frac{dz}{d\tau} \right) = 2\check{U}(x, y, z) - \left(\left(\frac{dx}{d\tau} \right)^2 + \left(\frac{dy}{d\tau} \right)^2 + \left(\frac{dz}{d\tau} \right)^2 \right) \quad (33)$$

Re-arranging Eq.(33), the zero-velocity surfaces can be found by setting $C(x, y, z, 0,0,0) = 2\check{U}(x, y, z) = C_0$. The Lagrangian points for the binary asteroid system can be found in pages 55-61 in Reference 24.

RESULTS

Binary Asteroid System in a Mutual Orbit

The physical parameters of 1999 KW4, which include the orbital elements, asteroid body dimensions and rotational rates, are used as nominal parameters for the two-ellipsoid binary asteroid bodies analyzed in this paper. The validation of the binary asteroid system models is based on the similarity of the of the orbital dynamics of asteroid bodies that have the same parameters as 1999 KW4, shown in Table 1 and Table 2.

Table 3 presents nondimensionalization parameters and Table 4 presents the initial state of the binary system.

Table 3. Nondimensionalization Parameters.

l	2547 m
r_0	766 m
v	0.9457

Table 4. Initial Parameters of the Binary Asteroid System Simulations.

	$\therefore = \tau$ (non-dimensional)	$\therefore = t$
$u _{\therefore=0}$	0.99915	2549 m
$\theta; \alpha_1; \alpha_2 _{\therefore=0}$	0	0
$\frac{d\theta}{d\therefore} \Big _{\therefore=0}$	1.0030	17.4 hr
$\frac{d\alpha_1}{d\therefore} \Big _{\therefore=0}$	5.4502	2.7 hr
$\frac{d u}{d\therefore}; \frac{d\alpha_2}{d\therefore} \Big _{\therefore=0}$	0	0

The Ellipsoid-Ellipsoid System. The dimensions of the two-ellipsoid system are the same as the 1999 KW4 system. The radii gyration of the asteroid bodies in Table 5 is computed by using Eqs. (9) to (12) and

Table 1. The initial non-dimensional parameter $u|_{\tau=0}=0.99915$ guarantees a mutual orbit similar to the orbital parameters of 1999 KW4 given in Table 2.

Table 5. Radii Gyration of the Ellipsoid-Ellipsoid System.

	Asteroid 1	Asteroid 2
P_{xx}	0.5878	0.1697
P_{yy}	0.5957	0.1958
P_{zz}	0.6251	0.2150

Figure 2 to Figure 5 present numerical simulations of the two-ellipsoid system for a total duration of $\tau_{tot} = 4 \times 2\pi$.

As illustrated in Figure 2, the two-ellipsoid asteroid bodies move in a nearly circular orbit. The maximum distance between the asteroid bodies is $\approx 2549 m$ and the minimum is $\approx 2547 m$, which are the actual apogee and perigee distance of the binary system 1999 KW4 (see Table 2).

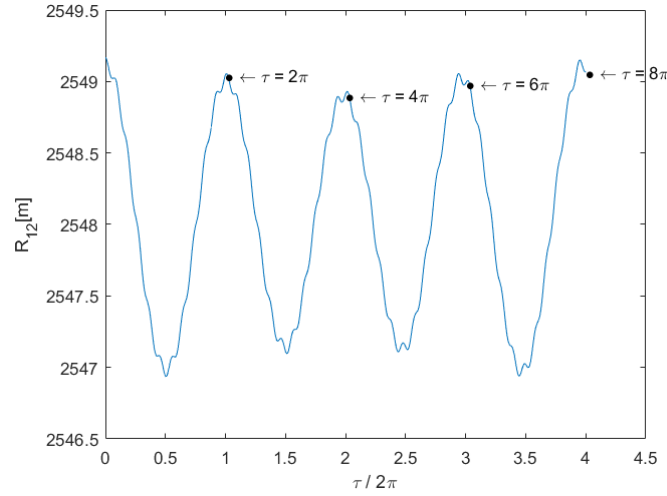


Figure 2. Distance between the two-ellipsoid bodies.

As shown in Figure 3 and Figure 4, the inertial rotational rate of the binary system and the local rotational rate of the primary body have high frequency oscillations but small amplitude variations of $1.003 < \frac{d\theta}{d\tau} < 1.005$ and $5.4475 < \frac{d\alpha_1}{d\tau} < 5.4505$, respectively.

In Figure 5, the orientation of the secondary body in the local reference frame remains relatively constant, i.e., the secondary asteroid body rotation is synchronous with the orbital motion of the binary asteroid, similar to the 1999 KW4 system.

For the two-ellipsoid system, the condition for energetic stability is a maximum $u_{max}^2(\tau) < 2.69$ and for Hill stability it is $u_{max}^2(\tau) < 10.01$ (see Eqs. (19) and (20) and Reference 25). Figure 6 presents the non-dimensional distance between the two-ellipsoid bodies $u(\tau)$ for a total duration of $\tau_{tot} = 100 \times 2\pi$.

The $u_{max}^2 \approx 1.0001$ of the two-ellipsoid system satisfies considerably the conditions for energetic stability and Hill stability. This means that the system has reached its lowest energy state and will remain bounded.

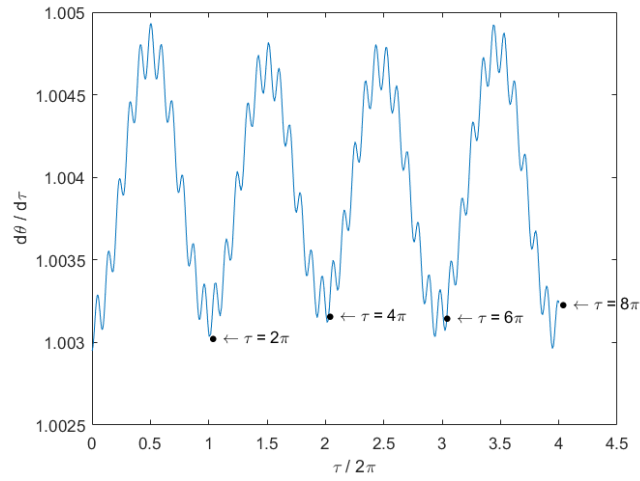


Figure 3. Inertial rotational rate of the two-ellipsoid binary system.

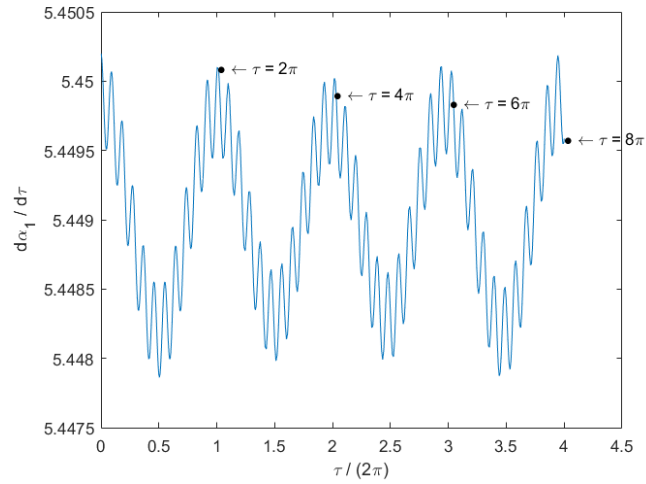


Figure 4. Local rotational rate of the ellipsoid primary body.

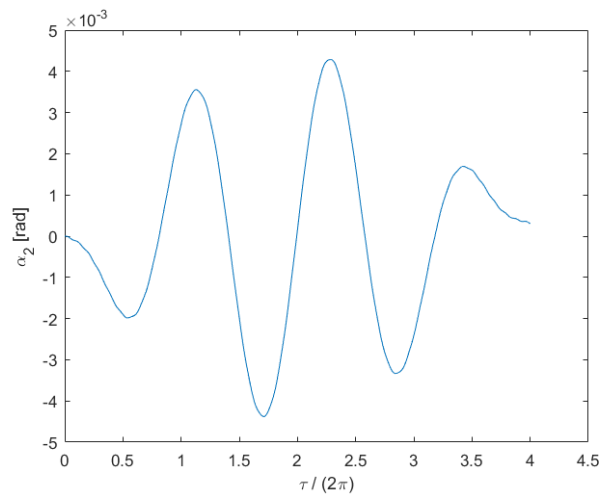


Figure 5. The orientation of the secondary body in the local reference frame.

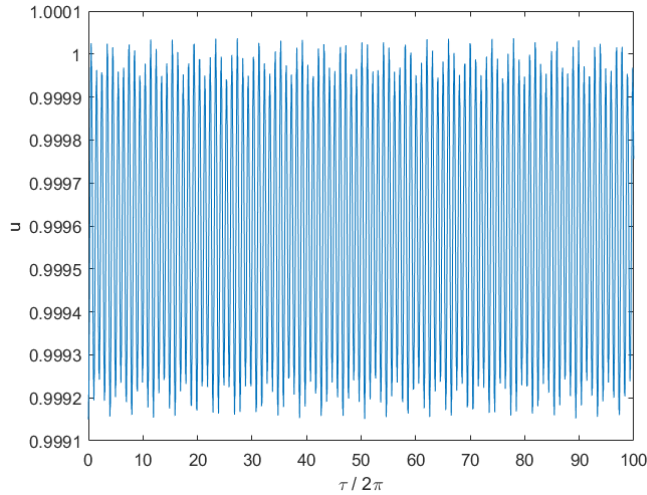


Figure 6. The nondimensional distance between the two-ellipsoid bodies.

Search for Stable Orbits around the Binary Asteroid System

The search for stable orbits around the two binary asteroid systems consists of varying the initial conditions of the spacecraft around the binary system and mapping the three possible outcomes: a) Collision with one of the asteroids; b) Escape from the gravitational influence of the binary system; c) A stable orbit that will not collide or escape the system for a given amount of time.

The solar radiation pressure is not considered in the grid method search because it requires more computational effort and the grid search method itself is time-consuming. The solar radiation pressure is considered when specified.

The Initial Keplerian Orbits around the Binary Asteroid System. This first search consists of positioning the spacecraft on an initial Keplerian orbit around the primary body. The orbit of the spacecraft does not remain in a Keplerian orbit for two reasons: the irregular shape of the primary asteroid body and the gravitational perturbation of the secondary asteroid body. Additionally, the solar radiation pressure is a non-conservative force that also disturbs the orbit.

Nevertheless, this method is useful for finding stable orbits when the primary body is much more massive than the secondary. The orbits far from the binary system that encompass both of the asteroid bodies considers the center of mass between the asteroid bodies as the focus of the orbit and the total mass of the binary system for the initial Keplerian elements.

The mapping is computed by varying two initial Keplerian elements: the semi-major axis and the eccentricity variation in Figure 8. The inclination of the orbit is 180° . Retrograde orbits are more stable than prograde orbits and for that reason a retrograde orbit was chosen.²⁶ The true anomaly is also 180° because it was found that there are more stable orbits with this true anomaly value. The ascending node and the argument of perigee are all zeroed.

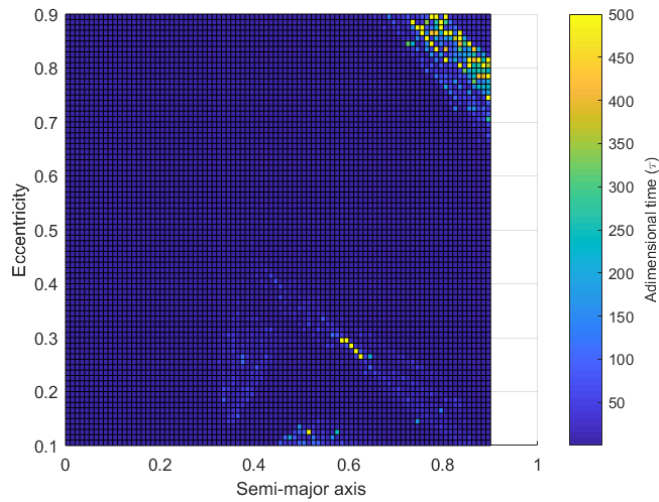


Figure 7. Search for stable orbits varying the semi-major axis and eccentricity initial values.

Figure 7 shows two bands of stable orbits, i.e., orbits that do not escape or collide with the asteroid bodies for $\tau = 500$. The larger band is studied in more detail in Figure 8, while the smaller, thinner band is studied in Figure 9.

Figure 8 presents highly eccentric initial Keplerian elements and large enough semi-major axes that they englobe both asteroids around the spacecraft's orbit (see Figure 10). The evolution of the orbital dynamics is shown in Figure 8b). Most of the non-stable orbits escape from the system. There is only one orbit that collides with the primary body in blue.

Figure 9 shows a stable orbit band around the primary asteroid body. Most of the orbits around stable orbits collide with the secondary body, but there are some that collide with the primary and a couple that escape the system.

Figure 10 presents a stable orbit from Figure 8 when $a = 0.85$ and $e = 0.82$ for an integration period $\tau = 10^3$ or $t \approx 116$ days.

The solar radiation pressure perturbation has a great influence on the orbital dynamics of the spacecraft. The main effect of the solar radiation pressure perturbation occurs at the perpendicular axis of the initial orbital plane (Z axis), as shown in Figure 11.

Figure 12 presents a stable orbit around the primary body from Figure 9 when $a = 0.6$ and $e = 0.275$. The simulation is for $\tau = 10^3$.

The solar radiation pressure in Figure 12 produces a great impact on the orbital dynamics. The effects of the solar radiation pressure on the spacecraft's orbit are noticeable and it should not be neglected for long binary asteroid systems missions.

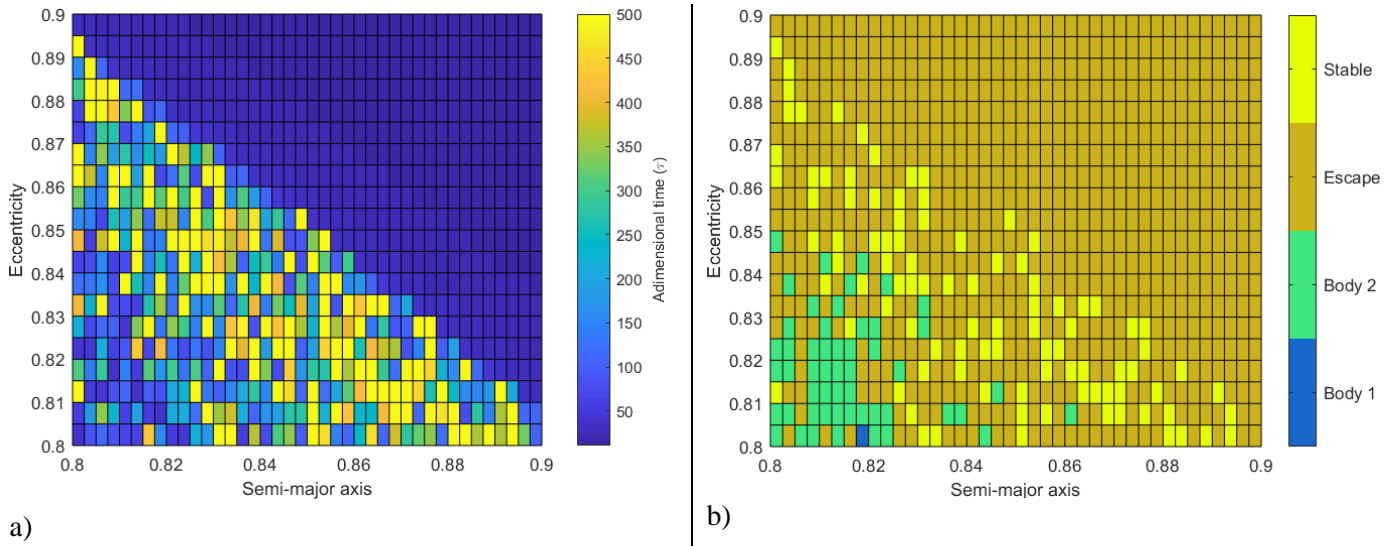


Figure 8. Search for stable orbits for highly eccentric initial state.

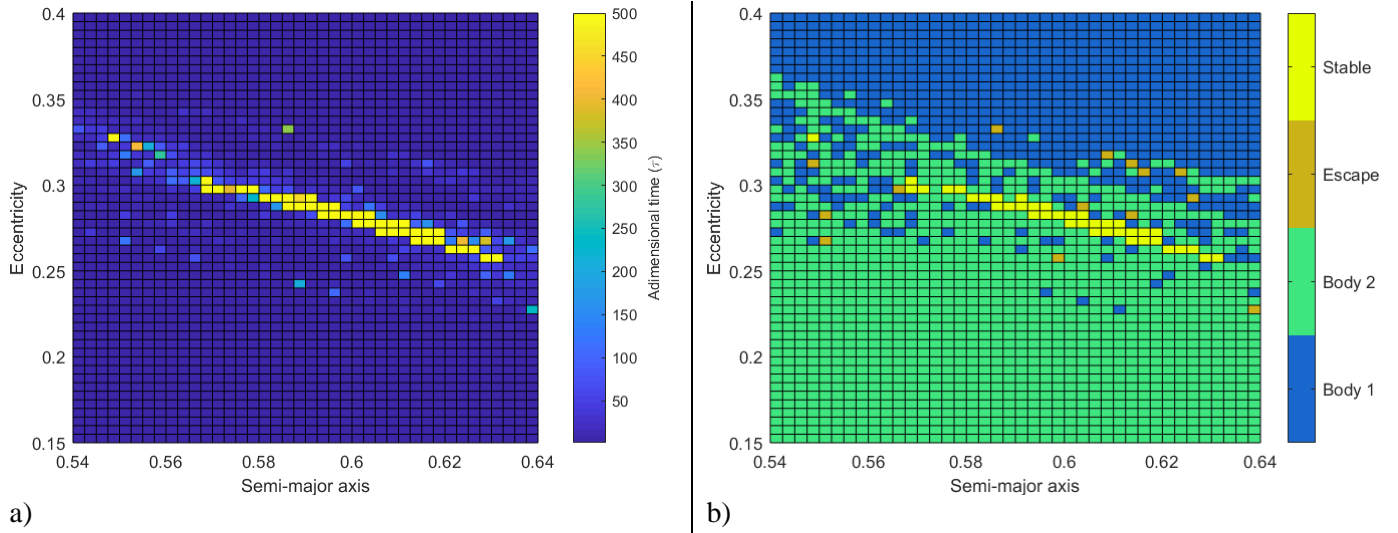


Figure 9. Search for stable orbits around the primary asteroid body.

All the simulations in this paper consider the initial state of the center of mass of the binary asteroid system to be in the perihelion of the orbit, when the true anomaly is 0° . According to Table 2, the highly eccentric orbit of the center of mass of the system provides a close approximation with the Sun, and therefore leads to an increase in solar radiation pressure perturbation.

Figure 13 compares the magnitude of the solar radiation pressure perturbation between the perihelion and the aphelion by subtracting the position of the spacecraft with and without the solar radiation pressure.

The acceleration force of the solar radiation pressure is inversely proportional to the square of the spacecraft's distance from the Sun. The difference between the solar radiation pressure perturbation magnitude at the perihelion and aphelion of the orbit is evident.

Figure 17 shows an initial inclination orbit of 90° for a stable orbit in

Figure 15. The orange orbit considers the solar radiation pressure, while the blue orbit does not consider any perturbation other than the non-sphericity of the asteroid bodies. As shown in Figure 17, the solar radiation pressure can change the orbit drastically. This orbit collides with the secondary body when $\tau = 350.9$.

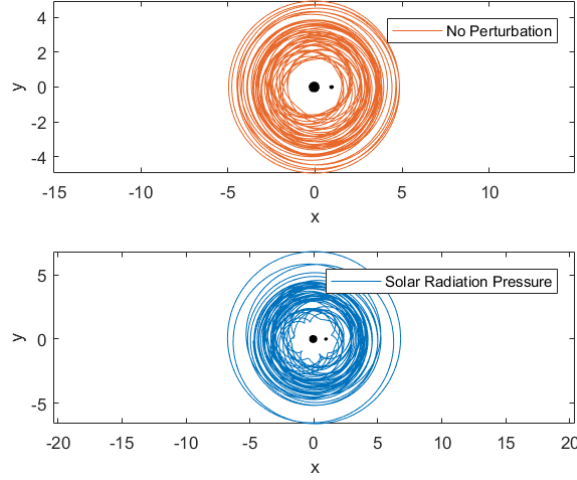


Figure 10. Spacecraft's stable orbit system with and without solar radiation pressure.

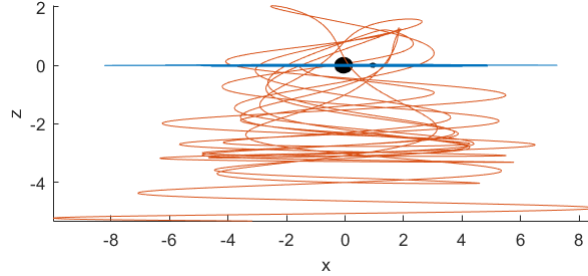


Figure 11. Spacecraft's stable orbit XZ axes view with (orange) and without (blue) solar radiation pressure for $\tau = 100$.

Figure 14 considers a true anomaly of 0° for the secondary asteroid body. The other initial Keplerian elements are kept the same as the previous simulation. The initial position of the spacecraft around the orbital binary system plane can be an important factor when searching for stable orbits (compare Figure 7 and 14). There is no stable orbit (with $\tau \geq 500$) in Figure 14 when the initial true anomaly is 0° .

Figures 15 and 16 consider a zeroed argument of perigee, ascending node angles, and 180° for true anomaly. The initial inclination is 90° in Figure 15 and 0° for Figure 16. The inclination can also be a crucial factor in finding stable orbits and is studied widely in the literature. there are more retrograde stable orbits around asteroid system than prograde orbits (compare Figure 7, 15 and 16 and see Reference 26). There are no stable orbits (with $\tau \geq 500$) in Figure 16 when the initial inclination is 0° .

Zero Velocity Curves. For second method used to search for stable orbits, it is assumed that the asteroid bodies orbit is in a mutual circular orbit (see Reference Roy). This assumption can be used for the KW4 because the binary system mutual orbit is nearly circular with an eccentricity of 0.0004.

Let the initial conditions of the spacecraft be $x|_{\tau=0} = x_c$, $y = z = dx/d\tau = dz/d\tau|_{\tau=0} = 0$. Then, a specific value of the Jacobi constant C_0 is chosen. The initial velocity $dy/d\tau|_{\tau=0}$ can be written as:

$$\left. \frac{dy}{d\tau} \right|_{\tau=0} = (2\tilde{U}(x_c, \vartheta_c, u_c) - C_0)^{1/2} \quad (34)$$

Based on the mathematical formulation of 24, the Lagrangian points of the binary two-ellipsoid system are: $L_1 = [0.6792, 0]$, $L_2 = [1.1953, 0]$, $L_3 = [-0.9887, 0]$, $L_4 = [0.4192, 0.8897]$ and $L_5 = [0.4192, -0.8897]$.

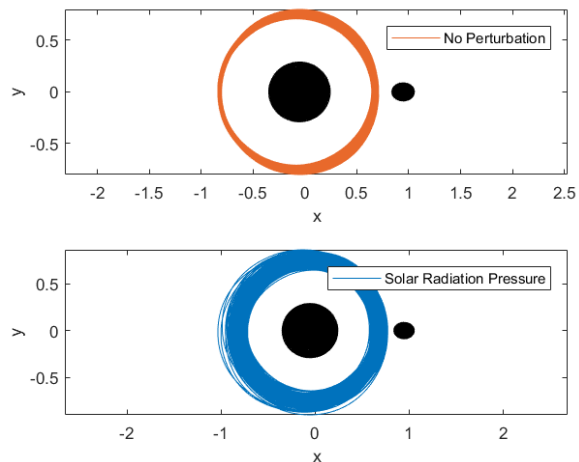


Figure 12. Spacecraft's stable orbit around the primary asteroid body with and without solar radiation pressure.

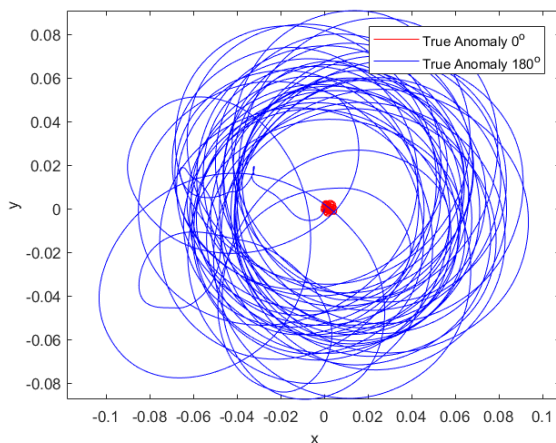


Figure 13. Difference between the position of the spacecraft with and without the solar radiation pressure.

The Jacobi constants for each Lagrangian point are: $C_{L1} = 3.48$, $C_{L2} = 3.39$, $C_{L3} = 3.07$, $C_{L4} = C_{L5} = 2.95$.

Let $C_0 = 3.7$ and $x|_{\tau=0} = -0.785$. The allowable region of the spacecraft's trajectory when $C_0 > C_{L1}$ and $x|_{\tau=0} = -0.785$ is around the secondary body as shown in Figure 18. According to Equation (34), $dy/d\tau|_{\tau=0} = 0.8250$. The initial state corresponds to a retrograde orbit.

The 3D orbit view is shown in Figure (20 for $\tau = 500$ and the comparison of the orbits with and without solar radiation pressure is given by Figure 19 for $\tau = 75$. The solar radiation pressure perturbation leads to a collision course with the secondary body when $\tau = 75$.

Let $C_0 = 2.95$ and $x|_{\tau=0} = -1.2$. The Jacobi constant $C_0 = C_{L4}$ results in an allowable region that englobes the binary system, except for the Lagrangian points L_4 and L_5 . Figure 19 shows the orbit with these initial parameters. The trajectory does not cross the Lagrangian points L_4 and L_5 . The solar radiation pressure perturbation plays an important role on the orbital dynamics of the spacecraft.

The analytical method to find stable orbits based on the Jacobi constant and Equation (34) cannot always find stable orbits. This method is good for finding orbits within a certain region, especially when the region is closed, e.g. $C_0 > C_{L1}$. But it cannot guarantee that a collision with the asteroid bodies will be avoided. The grid method or the mapping method combined with the Jacobi constant can be a useful tool to find the stable orbits in restricted allowable trajectory paths. Figure 21 combines the Jacobi method in Equation (34) and the grid method to find stable orbits ($\tau = 100$).

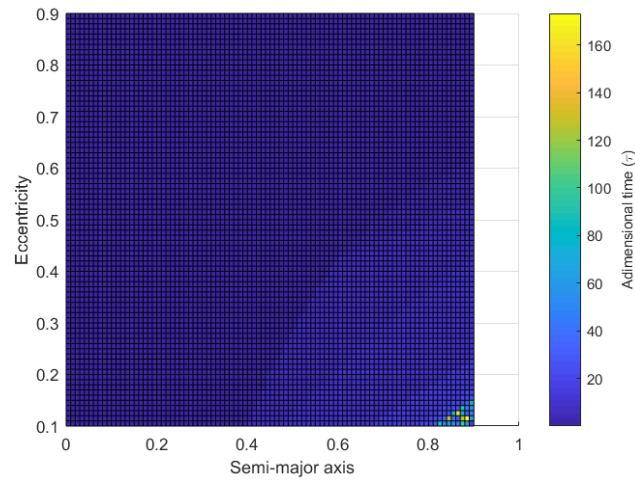


Figure 14. Search for stable orbits with zeroed true anomaly and varied varying the semi-major axis and eccentricity.

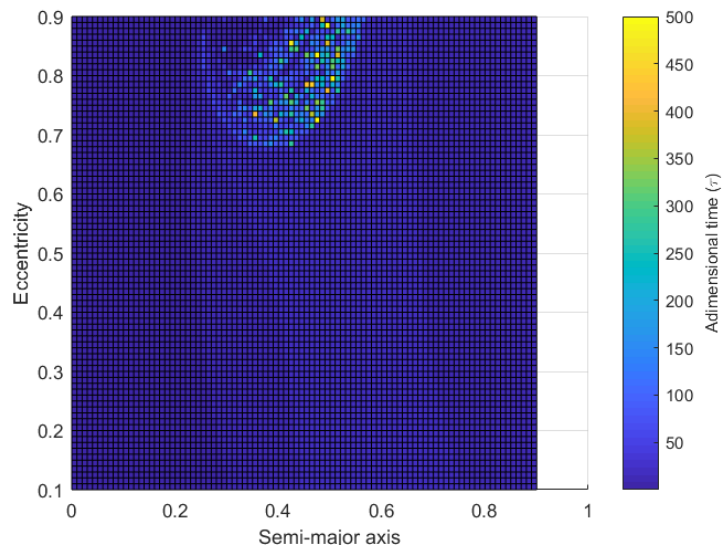


Figure 15. Search for stable orbits with 90° inclination, and varied the semi-major axis and eccentricity initial values.

The stable orbits shown in Figures 20 and 21 can be seen in Figure 34 with the initial Jacobi constant and the initial position of the spacecraft. Note that the initial positions are all negative because there are more stable orbits in this geometry (see Figure 7 and Figure 14).

In Figure 21, the blue vertical band occurs for one or both of the following reasons: the secondary asteroid body is in a collision path with spacecraft; and/or it is non-allowable region for the spacecraft to be, according to

the Jacobi constant. Figure 23 is useful for finding stable orbits around a certain allowable region that the spacecraft can orbit, based on the Jacobi constant.

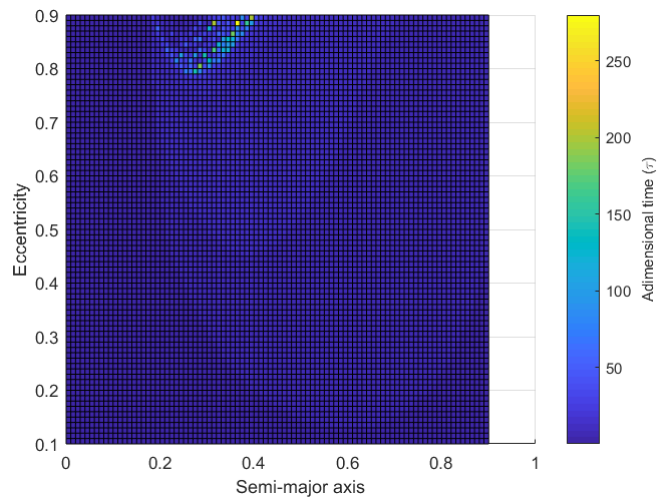


Figure 16. Search for stable orbits with zeroed inclination, and varied semi-major axis and eccentricity initial values.

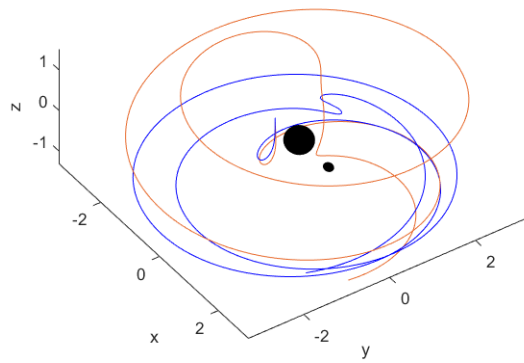


Figure 17. Search for stable orbits with zeroed inclination, and varied the semi-major axis and eccentricity initial values.

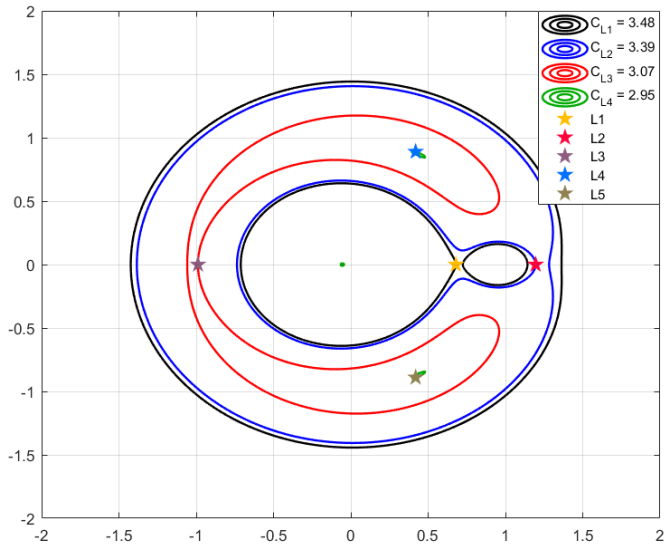


Figure 18. Zero Velocity Curves and Lagrangian Points.

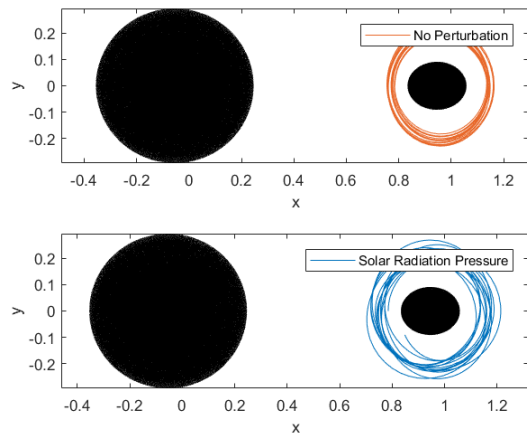


Figure 19. Spacecraft's stable orbit around the primary asteroid body with and without solar radiation pressure.

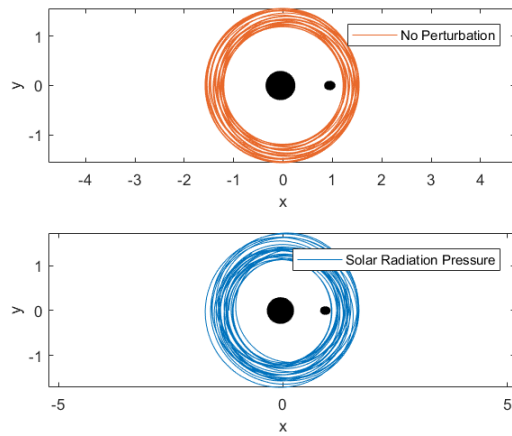


Figure 20. Spacecraft’s stable orbit around the binary asteroid system with and without solar radiation pressure.

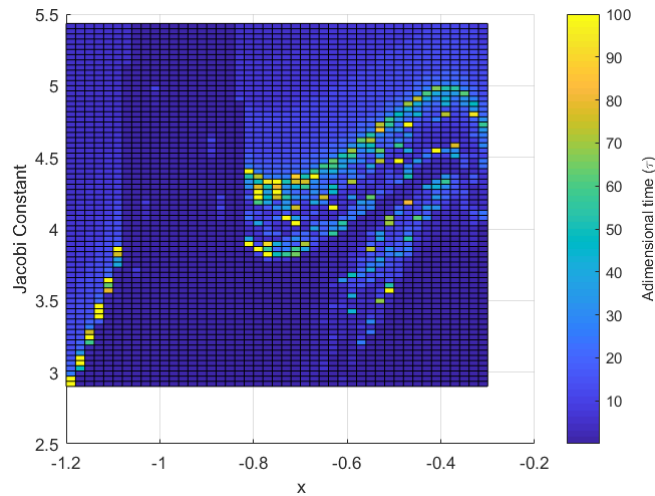


Figure 21. Search for stable orbits varying the Jacobi constant and the initial position of the spacecraft.

CONCLUSION

The two-ellipsoid system considered in this paper’s results has similar dynamics to the real KW4 binary system as presented in the literature review. The system is stable, i.e., the asteroid bodies do not collide with each other, do not escape from the system, and not seek out a lower energy state.

The grid method can find several stable orbits. The maps can show regions where there are a great number of stable orbits, or where a potential external perturbation may not destabilize the system as easily as a region where there are few stable orbits.

The Keplerian elements or Keplerian orbit method for finding stable orbits is efficient. This method is great for binary systems in which the primary body is much more massive than the secondary body (moonlet).

The Jacobi Constant method for finding stable orbits is also capable of finding a great spectrum of stable orbits. The greatest advantage to using this method with the grid search is that it is easy to visualize the allowable regions that the spacecraft can be. In this way, it is easy to find stable orbits around the primary or secondary asteroid body.

The solar radiation pressure magnitude in the perihelion of the orbit is noticeable and will eventually require a control system to correct the spacecraft’s orbit. The magnitude of the solar radiation pressure at the aphelion of the orbit is much less intense.

ACKNOWLEDGMENTS

The authors wish to express their appreciation for the support provided by grants 406841/2016-0 and 301338/2016-7 from the National Council for Scientific and Technological Development (CNPq), and grants 2016/14665-2, 2016/18418-0, 2017/07539-3 from São Paulo Research Foundation (FAPESP). We are also grateful for the financial support from the National Council for the Improvement of Higher Education (CAPES) and thanks to John Bradford Tarley for proofreading the article.

REFERENCES

- ¹ Pfalzner, S. The Formation of the Solar System. *Physica Scripta*, Vol. 90, No. 6, 2015, 18 pp. DOI:10.1088/0031-8949/90/6/06800
- ² NASA. Solar System Exploration. Small Bodies. Asteroids. <https://solarsystem.nasa.gov/small-bodies/asteroids/in-depth>, December 2017. Accessed: June 2018.
- ³ Phys.org. Astronomy and Space Exploration. <https://phys.org/news/2016-11-smallest-asteroid-characterized-earth-based-telescopes.html>, November 2016. Accessed: June 2018.
- ⁴ Vishnu, R. et al., Physical Characterization Of ~2 M Diameter Near-Earth Asteroid 2015 Tc25: A Possible Boulder From E-Type Asteroid (44) Nysa, *The Astronomical Journal*, Vol. 152:162, 2016, 7pp. DOI: 10.3847/0004-6256/152/6/162
- ⁵ Thomson, K. S., Explanation of large scale extinctions of lower vertebrates, *Nature*, Vol. 261, 1976, pp. 578-580. DOI:10.1038/261578a0.
- ⁶ Kawaguchi J., Fujiwara A. and Uesugi T. Hayabusa—Its technology and science accomplishment summary and Hayabusa-2. *Acta Astronautica*, Vol. 62, No. 10-11, 2008, pp. 639-647. <https://doi.org/10.1016/j.actaastro.2008.01.028>
- ⁷ Michel, P., et al. Science case for the Asteroid Impact Mission (AIM): A component of the Asteroid Impact & Deflection Assessment (AIDA) mission. *Advances in Space Research*, 2016, pp. 19. <http://dx.doi.org/10.1016/j.asr.2016.03.031>
- ⁸ Sukhanov, A. A., Velho H. F. C., Macau, E. E. N. and Winter, O. C. The Aster Project: Flight to a Near-Earth Asteroid. *Cosmic Research*. Vol. 48. No. 5. 2010, pp. 443-450. DOI:10.1134/S0010952510050114.
- ⁹ Araujo, R. A. N., Winter, O. C., Prado, A. F. B. A. Stable retrograde orbits around the triple system 2001 SN263. *Monthly Notices Of The Royal Astronomical Society*, Vol. 449, No. 4, 2015, pp. 4404-4414. Available in: <<http://hdl.handle.net/11449/129864>>.
- ¹⁰ Belton, M. J. S., et al., The Discovery and Orbit of 1993 (243)1 Dactyl, *Icarus*, Vol. 120, No. 1, 1996, pp. 185-199. <https://doi.org/10.1006/icar.1996.0044>.
- ¹¹ Asteroids with Satellites by Johnston, W. R. Asteroids with Satellites. <http://www.johnstonsarchive.net/astro/asteroidmoons.html>, July 2018. Accessed: July 2018.
- ¹² Pravec, P. et al. Binary asteroid population. 3. Secondary rotations and elongations, *Icarus*, Vol. 267, 2016, pp. 267-295. <https://doi.org/10.1016/j.icarus.2015.12.019>.
- ¹³ Margot, J. L., Pravec, P., Taylor, P., Carry, B., and Jacobson, S. Asteroid systems: Binaries, triples, and pairs, *In Asteroids IV*, 2015, pp. 355-374. DOI: 10.2458/azu uapress 9780816532131-ch019.
- ¹⁴ Pravec, P. et al. Photometric survey of binary near-Earth asteroids, *Icarus*, Vol. 181, 2006, pp. 63-93.
- ¹⁵ Ticha, J. et al., 1999 KW4, *Minor Planet Electronic Circ.*, Vol. 1999-K28, 1999.
- ¹⁶ Ostro, S. J. et al. Radar Imaging of Binary Near-Earth Asteroid (66391) 1999 KW4. *Science*, Vol. 314, 2006, pp. 1276-1280. DOI: 10.1126/science.1133622.
- ¹⁷ Bellerose, J. and Scheeres, D. J. Restricted Full Three-Body Problem: Application to Binary System 1999 KW4, *Journal of Guidance, Control and Dynamics*, Vol. 31, No. 1, 2008. DOI: 10.2514/1.30937
- ¹⁸ Scheeres, D. J. et al. Dynamical Configuration of Binary Near-Earth Asteroid (66391) 1999 KW4, *Science*, Vol. 314, No. 5803, 2006, pp. 1280-1283. DOI: 10.1126/science.1133599
- ¹⁹ Howell, K. and Chappaz, L. Bounded Orbits near Binary Systems Comprised of Small Irregular Bodies. AIAA/AAS Astrodynamics Specialist Conference, 2014. DOI: 10.2514/6.2014-4153
- ²⁰ Milani, A., Nobili, A. M. and Farinella, P. Non-gravitational Perturbations and Satellite Geodesy. Dipartimento di Matematica, Universita di Pisa, 1st ed., 1987, 456 pp. ISBN-13: 978-0852745380
- ²¹ Lyon, R.H. Geosynchronous orbit determination using space surveillance network observations and improved radiative force modeling, Thesis, Massachusetts Institute of Technology, Dept. of Aeronautics and Astronautics, 2004, 375 p. URI: <http://hdl.handle.net/1721.1/17779>
- ²² Luthcke, S. B. et al. Enhanced Radiative Force Modeling of the Tracking and Data Relay Satellites. *The Journal of the Astronautical Sciences*, Vol. 45, No. 3, 1997, pp 349-370.

- ²³ Kubo-oka, T. and Sengoku, A. Solar Radiation Pressure Model for the Relay Satellite of SELENE. *Earth, Planets and Space*, Vol. 51, 2004, pp. 979-986. <https://doi.org/10.1186/BF03351568>
- ²⁴ Woo, P. Dynamics of a Spacecraft in the vicinity of a Binary Asteroid System. Thesis. McGill University, Dept. of Mechanical Engineering, 2004.
- ²⁵ Schreeres, D. J. Stability of the planar full 2-body problem. *Celestial Mechanics Dynamical. Astronomy*, Vol: 104, 2009, pp. 103-120. DOI 10.1007/s10569-009-9184-7
- ²⁶ Moulton, F. R. On the Stability of Direct and Retrograde Satellite Orbits. *Monthly Notices of the Royal Astronomical Society*, Vol: 75, No:2, pp. 40-57, 1914. <https://doi.org/10.1093/mnras/75.2.40>
- ²⁷ Roy, A. E. *Orbital Motion*. Institute of Physics Publishing, Bristol, 4th ed., 2005.